Organic & Biomolecular Chemistry

Dynamic Article Links

Cite this: *Org. Biomol. Chem.*, 2011, **9**, 7151

www.rsc.org/obc

PAPER

Silent, fluorescent labeling of native neuronal receptors†

Devaiah Vytla,[a] Rosamund E. Combs-Bachmann,[b] Amanda M. Hussey,[a] Ismail Hafez[c] and James J. Chambers*[a,b]

Received 14th June 2011, Accepted 4th August 2011
DOI: 10.1039/c1ob05963g

We have developed a minimally-perturbing strategy that enables labeling and subcellular visualization of endogenous dendritic receptors on live, wild-type neurons. Specifically, calcium-permeable non-NMDA glutamate receptors expressed in hippocampal neurons can be targeted with this novel synthetic tri-functional molecule. This ligand-directed probe was targeted towards AMPA receptors and bears an electrophilic group for covalent bond formation with an amino acid side chain on the extracellular side of the ion channel. This molecule was designed in such a way that the use-dependent, polyamine-based ligand accumulates the chemically-reactive group at the extracellular side of these polyamine-sensitive receptors, thereby allowing covalent bond formation between an electrophilic moiety on the nanoprobe and a nucleophilic amino acid sidechain on the receptor. Bioconjugation of this molecule results in a stable covalent bond between the nanoprobe and the target receptor. Subsequent photolysis of a portion of the nanoprobe may then be employed to effect ligand release allowing the receptor to re-enter the non-liganded state, all the while retaining the fluorescent beacon for visualization. This technology allows for rapid fluorescent labeling of native polyamine-sensitive receptors and further advances the field of fluorescent labeling of native biological molecules.

Introduction

AMPA receptors play a critical role in long-term potentiation (LTP), one of the mechanisms thought to underlie memory formation at the cellular and molecular level. The ability to image these receptors without perturbing receptor activity is crucial to gaining a better understanding of these processes. A subset of AMPA receptors that are currently of considerable interest are those that lack the GluA2 subunit, which renders them calcium-permeable.[1] The precise role of these receptors in synaptic plasticity has yet to be elucidated and is the subject of ongoing debate in the field. Here we present a novel photo-cleavable nanoprobe for labeling native, calcium-permeable non-NMDA glutamate receptors with minimal disruption to native activity.

Static and dynamic protein localization studies of membrane-bound receptors typically involve an exogenously applied fluorescent tag or genetically encoded fluorescent protein to spatiotemporally monitor protein location. Currently, popular approaches to specifically co-localize a fluorophore with a protein of interest are overexpression of a fluorescent protein fused to a target protein or the application of an antibody to a protein of interest.[2,3] Overexpression relies on the introduction of a gene construct encoding the protein fused to either a fluorescent protein such as GFP[4] or a small peptide affinity tag that specifically binds to a fluorescent probe such as the recently-developed FlAsH or Snap-Tag systems.[5–8] Though genetically-encoded fluorescent reporters of receptor dynamics have become commonplace in biology, over-expression of tagged-monomeric subunits of heteromultimeric proteins have been observed to bias receptor subtype composition and function thus potentially confounding experimental results.[9–11]

In contrast, the antibody method of labeling native receptors typically requires the addition of large proteinaceous molecules to track the movement of receptors. This latter method offers the benefit of exquisite specificity towards the endogenous protein of interest, however the large size of typical antibodies combined with the size of typical fluorescently-tagged secondary antibodies may impose unforeseen consequences when studying natural protein movements on the cell surface. This is particularly important when studying movements of receptors into or out of the synapse, as the synaptic cleft is not much larger than an antibody/receptor complex.[12,13] Here we introduce a method for labeling native membrane-bound receptors in which we employ a small, non-perturbing molecule to covalently label native receptors with a fluorescent marker that then allows observation of these receptors using standard epifluorescence microscopy.

This low molecular weight probe consists of a photolabile, tri-functional molecule that is chemically engendered with a

[a]*Department of Chemistry, University of Massachusetts Amherst, Amherst, MA 01003, USA*
[b]*Neuroscience and Behavior Program, University of Massachusetts Amherst, Amherst, MA 01003, USA*
[c]*Department of Biochemistry and Molecular Biology, and Brain Research Centre, University of British Columbia, British Columbia, Canada*
† Electronic supplementary information (ESI) available. See DOI: 10.1039/c1ob05963g

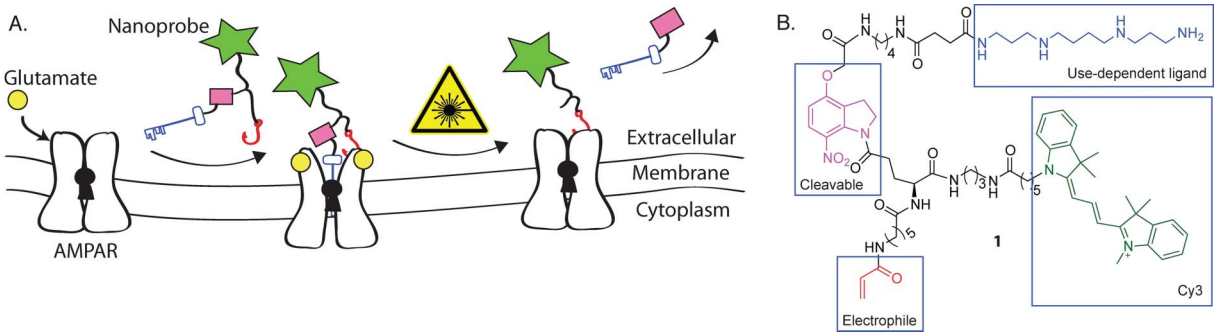

Fig. 1 Building a better molecular burr. A) Cartoon representation of nanoprobe concept. First, the nanoprobe interacts with a target binding site after presynaptically-released glutamate activates the ion channel. Next, the electrophilic moiety (red hook) and a biological nucleophile react to generate a new covalent linkage. Finally, light is used to photolytically-cleave the linker connecting the ligand (blue key), leaving the neurotransmitter receptor covalently labeled with a fluorophore (green star). B) Structure of nanoprobe **1**.

fluorescent reporter, a covalently-attached ligand, and a promiscuous electrophilic group for covalent bond formation with the target receptor (Fig. 1). The persistence of ligand activity may be terminated by photolysis of the branch connecting the ligand to the remainder of the molecule. This system makes use of the same methoxynitroindoline (MNI) chromophore that is involved with photolytic release of glutamate from MNI-glutamate.[14–16] After the tether connecting the ligand to the core of the molecule is photolytically cleaved, the ligand can diffuse away from the receptor, leaving the fluorophore covalently bound to the target receptor. The protein may then be observed with standard epifluorescence microscopy in an unbound, native state. It is important to relieve persistently-activated or antagonized receptors to avoid changes to the receptor which are accompanied by ligand binding. Agonist-induced conformational changes of several receptor types including glutamate receptors have been shown to induce clathrin-mediated endocytosis or differential trafficking patterns.[17–19] Antagonist-induced alterations in receptor trafficking have also been described.[20,21] These findings highlight the potential problem of using a ligand-based fluorophore such as glutamate covalently linked to a fluorescent molecule (*i.e.* fluorescein or a quantum dot) to label receptors. Due to the reliance on maintained receptor occupancy by glutamate during imaging, one would be able to observe only receptors in an occupied, and thus perturbed, state.

Proximity-accelerated reactivity: Tethered ligands have been used successfully to enhance the local reactivity of a variety of reactive groups on small molecular probes.[22–28] As the molecule diffuses through the buffer or extracellular milieu, binding events occur between the tethered ligand and a binding site on the target macromolecule as well as non-specific binding events between the molecule and non-target proteins. When the small molecule is bound to a high-affinity binding site and thus confined, the effect on the remainder of the molecule is an increase in effective concentration of the reactive group.[29] During the time that the ligand is bound to the target protein, the reactive electrophile on the small molecule is sequestered near a number of Michael addition-capable amino acid side chains normally present on the receptor. In analogous systems, the reaction between the side chains of the target and the electrophile is accelerated many hundred- to thousand-fold due to the reduced entropy of the bimolecular system.[22,30] Acrylamide (red hook in Fig. 1) has been incorporated in nanoprobe **1** through a flexible linker because of the known efficiency of reaction with biologically-presented nucleophiles.[30,31] Nucleophilic partners for reaction with this Michael acceptor may be any one of several naturally-occurring amino acid residues that are located near the binding site (cysteine, serine, threonine, tyrosine, and possibly lysine[32]) ensuring a multitude of potential reactive sites on endogenous and heterogeneous receptor populations. The targeting ligand in nanoprobe **1**, a functionalized polyamine similar to that found in naphthylacetylspermine (NASPM) or Joro spider toxin, is known to act as a use-dependent blocker of active, calcium-permeable non-NMDA glutamate receptors.[33–36] These functionalized polyamines are part of a different pharmacological class from the typical, endogenous polyamines that modulate inward rectification of certain ion channels.

Results and discussion

Chemistry

Borrowing from a synthetic precedent,[37] the nitroindoline core was synthesized and elaborated synthetically to offer three orthogonal protecting groups to allow for further chemical modification (Scheme 1). The three functional parts as well as the photolabile nitroindoline core of nanoprobe **1** were synthesized separately and assembled together in a convergent fashion. The synthesis of core nitroindoline commenced with a literature precedent synthesis of **2**. Selective Boc-deprotection of **2** using dichloroacetic acid[38] afforded primary amine **3** that was then coupled to the carboxylic acid of previously-reported tethered acrylamide **4**[39] using HATU/HOAt and collidine to yield **5**. Next, *tert*-butyl ester **5** was treated with TFA to afford the carboxylic acid **6** and this was coupled to the amine-functionalized Cy3 **7**[40] using HATU/HOAt and collidine to afford **8**. The methyl ester of **8** was then hydrolyzed to afford compound **9**, a portion of which is used as a control molecule for electrophysiological and imaging experiments. Spermine was protected following a literature precedent[41] and then functionalized to afford compound **10** which was coupled to compound **9** with EDC to afford protected intermediate **11**. Subsequent deprotection using TFA afforded the final compound **1**.

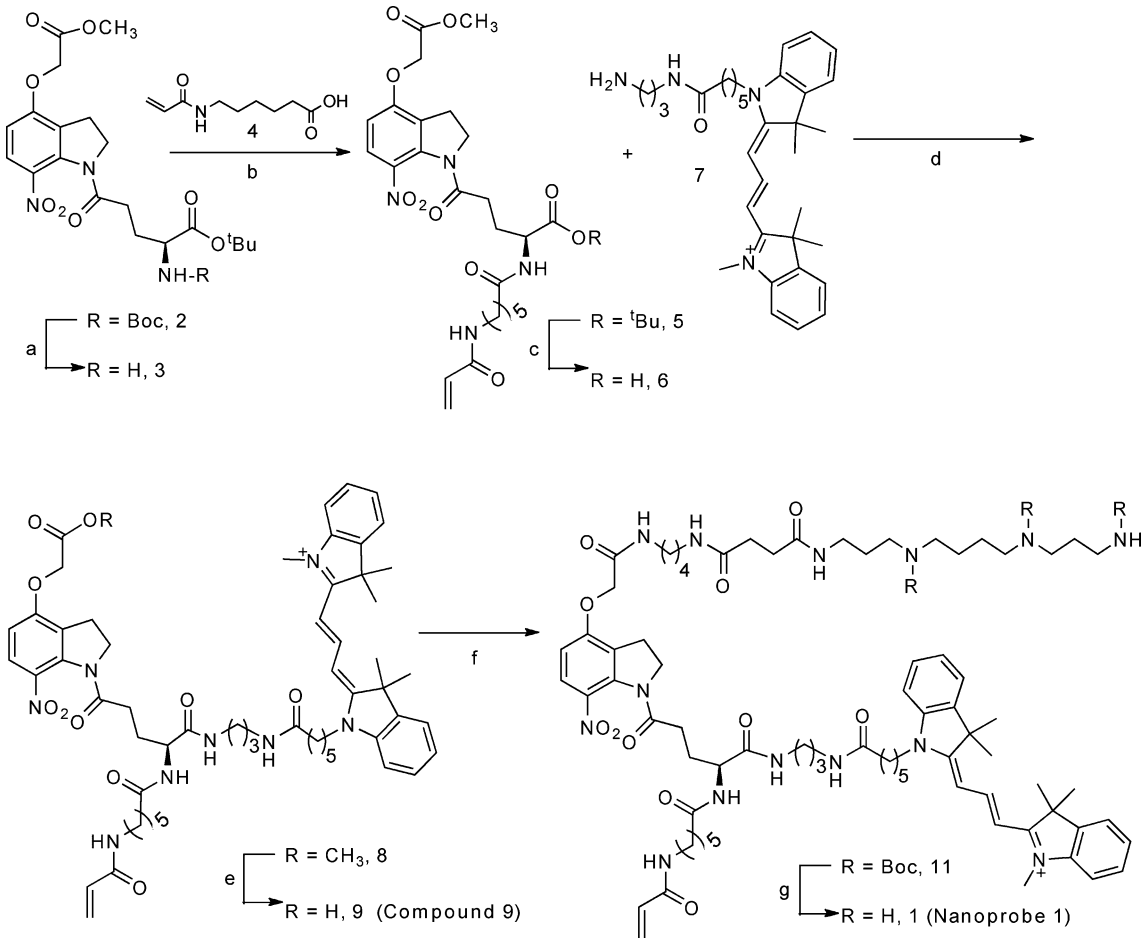

Scheme 1 Synthesis of nanoprobe **1**. *Reagents and conditions*: (a) $Cl_2CHCOOH : CH_2Cl_2$ (1 : 1), rt, 21 h, 91%; (b) HATU/HOAt, Collidine, DMF, rt, 21 h, 50%; (c) 10% TFA, CH_2Cl_2, rt, 12 h, 96%; (d) HATU/HOAt, Collidine, DMF, rt, 24 h, 58%; (e) 1 N NaOH/MeOH, rt, 2 h, 97%; (f) **10**, EDC, CH_3CN : DMF (4 : 1), rt, 48 h, 56%; (g) 20% TFA in CH_2Cl_2 0 °C to rt, 30 min, 98%.

Biology

Patch clamp electrophysiology experiments performed on HEK293T cells heterologously expressing non-desensitizing GluA1-L497Y homomultimers demonstrate that 1 μM nanoprobe **1**, when co-applied with 20 μM glutamate, blocks approximately 60% of the glutamate-evoked current (Fig. 2) after short co-incubations in a fashion similar to other polyamine-based small molecules. NASPM, the polyamine ligand that served as the basis for our design, was found to have an IC_{50} of 0.33 μM at calcium-permeable AMPA receptors and blocked approximately 70% of agonist-evoked current at 1 μM.[36] In the case of nanoprobe **1**, the polyamine blockage may be released by irradiation of the test cell with violet light (380 nm), returning the channels to a native gating state as measured by patch clamp electrophysiology. In contrast, when these cells were incubated with 1 μM nanoprobe **1** without the addition of glutamate to the bath, approximately 20% blockage was measured. This observed pore blockage is likely due to the additional voltage-dependency of polyamine blockage coupled with stochastic channel opening of AMPA receptors.[36] These results suggest that like other functionalized polyamines, the efficiency of binding is enhanced through the use-dependent nature of the spermine ligand. Additionally, these experiments support the supposition that nanoprobe **1** indeed labels polyamine-sensitive receptors at excitatory synapses where glutamate is being released by presynaptic neurons. The nanoprobe system as evaluated in these electrophysiology experiments appears to behave as an affinity label that can then be rapidly cleaved with light to return the receptor to a normal gating state.

Live cell imaging experiments with primary dissociated hippocampal neuron cultures employing nanoprobe **1** demonstrate that this method does indeed target fluorescent imaging dyes to regions of the cells expected to harbor polyamine-sensitive and synaptically-active glutamate receptors. Cells were imaged with transmitted light and then serially with fluorescent light to acquire background data. Next, ligand-lacking compound **9** or ligand-containing nanoprobe **1** were applied to the cells in the dark to avoid premature photolysis. After incubation for 2 min, fluorescence imaging was resumed as washout occurred to remove non-bound dye. The images (Fig. 3) were obtained from dissociated primary hippocampal neurons that were incubated for 20–24 days. Cells were washed with extracellular recording buffer, incubated in 750 nM nanoprobe **1** or **9** for 2 min, and then perfused constantly with extracellular recording buffer. Since nanoprobe **1** contains a use-dependent ligand, we expected the Cy3 fluorescence to accumulate mainly to those receptors that

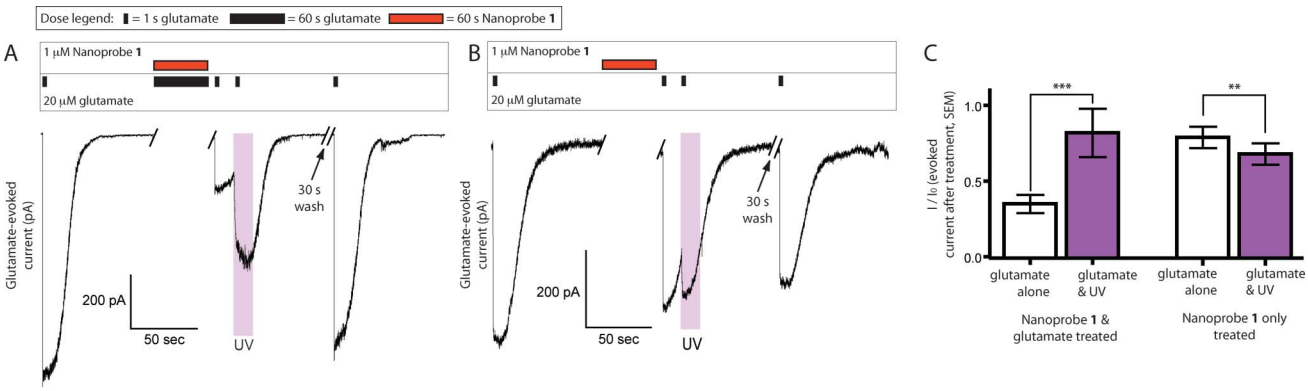

Fig. 2 Nanoprobe **1** behaves electrophysiologically as a photolabile blocker at GluA1-L497Y receptors. A) Representative patch clamp recording from a single HEK293T cell heterologously expressing GluA1 homomers demonstrating the effect of co-application of nanoprobe **1** and glutamate (1 μM for nanoprobe **1** and 20 μM for glutamate in all electrophysiology recordings). Glutamate-evoked current was measured before treatment (glutamate application times represented by black boxes above trace) and then glutamate *with* nanoprobe **1** was used to treat the cells for 1 min (co-application indicated by aligned black and red boxes above trace). Subsequent glutamate applications demonstrate a marked reduction in current and that a portion of the glutamate current can be immediately restored by photolysis of the linker connecting the ligand on nanoprobe **1** (purple area indicates UV light on). Finally, test treatments with glutamate on the same cell later in the recording demonstrate normal glutamate-evoked current. B) Representative patch clamp recording of glutamate-evoked current in a GluA1-expressing HEK293T cell. After measuring glutamate-evoked current, cells were treated with nanoprobe **1** (red box above trace) in the absence of glutamate for 1 min. Then glutamate-evoked current was measured before and after photolysis of the linker. For this control labeling, only a small reduction in current is observed confirming the use-dependency of nanoprobe **1**. Furthermore, response to glutamate after photolysis is less than the initial glutamate response that was not paired with UV light suggesting that the decrease in current may be due to something other than blockage by nanoprobe **1** (*i.e.* rundown of current during recordings or channel desensitization is commonly observed in experiments such as these). C) Quantification of normalized peak glutamate-evoked current before and after photolytic-release of ligand. The two left columns represent before and after photolytic-release of ligand on cells co-treated with nanoprobe **1** *and glutamate* ($n = 10$) and two right columns represent before and after photolytic-release of ligand on cells treated with nanoprobe **1** *alone* ($n = 6$). Data presented as mean and SEM (error bars). Photolytic-release in the nanoprobe **1** *and glutamate* co-treatment group demonstrates a significantly larger glutamate-evoked current after photolytic-release (***$P = 0.0007$, paired t-test).

are located at synaptic regions. These regions should be the main sites receiving basal glutamatergic release in the form of native chemical neurotransmission. Indeed we observed fluorescence accumulation at regions of the neuronal culture that appear to be synaptic spines based on the bright-field morphology. When incubated with non-liganded compound **9**, fluorescence that was present on or near the cells after treatment quickly washed away once perfusion was restarted. However, in the case of nanoprobe **1**, the accumulated fluorescence persists after washing and is still easily visible many minutes after continuous perfusion and imaging. This result suggests that nanoprobe **1** is indeed acting covalently and through a ligand-dependent reaction.

A large quantity of biological nucleophiles are present in and on cultured neurons and as such, one may expect a high degree of background reactivity between the acrylamide on our probes and a non-target protein. However, like other recently employed electrophile-containing molecules,[26,42] nanoprobe **1** is not a simple acrylamide. Thus, we have been able to apply our nanoprobe at a concentration that does not promiscuously label all biological nucleophiles, yet still reaches an effective concentration for reaction of the acrylamide and the target protein. Use of non-liganded molecule **9** demonstrates that the electrophilic portion of the molecule is not overly reactive towards the myriad available biological nucleophiles. Most certainly there are numerous off-target crosslinks that are made through chance encounters, but our imaging data from experiments with control compound **9** compared to nanoprobe **1** suggest that this is not a major result of the addition of this probe to cultured neurons.

Native hippocampal neurons express numerous types of polyamine-sensitive ion channels and the reaction between nanoprobe **1** and one of these other channels (kainite, NMDA, calcium-impermeable AMPA, *etc.*) cannot be ruled out given the relatively high concentration of nanoprobe **1** that was applied during the imaging experiments.[43] While spermine itself has been shown to potentiate NMDA receptors, the EC_{50} for voltage-independent, glycine-independent potentiation is about 150 μM.[44] The more relevant effects of NASPM, a synthetic analogue of Joro spider toxin, on NMDA receptors and calcium-impermeable AMPA receptors is less well understood as this is generally considered a specific blocker of calcium-permeable AMPA and kainate receptors.[36] Combined, electrophysiology and imaging results provide evidence that nanoprobe **1** labels native polyamine-sensitive non-NMDA receptors in live, primary hippocampal neuronal culture while leaving these receptors in an unbound state once the ligand has been photolytically-released.

Conclusion

The novel nanoprobe technology that we have introduced in this work offers a new technique to the ever-expanding toolbox available to cell biologists and, more specifically, neuroscientists. We have demonstrated the utility of a small molecular probe for the labeling in live cells of polyamine-sensitive ion channels thought to play a key role in learning and memory. This labeling approach offers a significantly smaller and easier method than those that are currently available to the community at large.

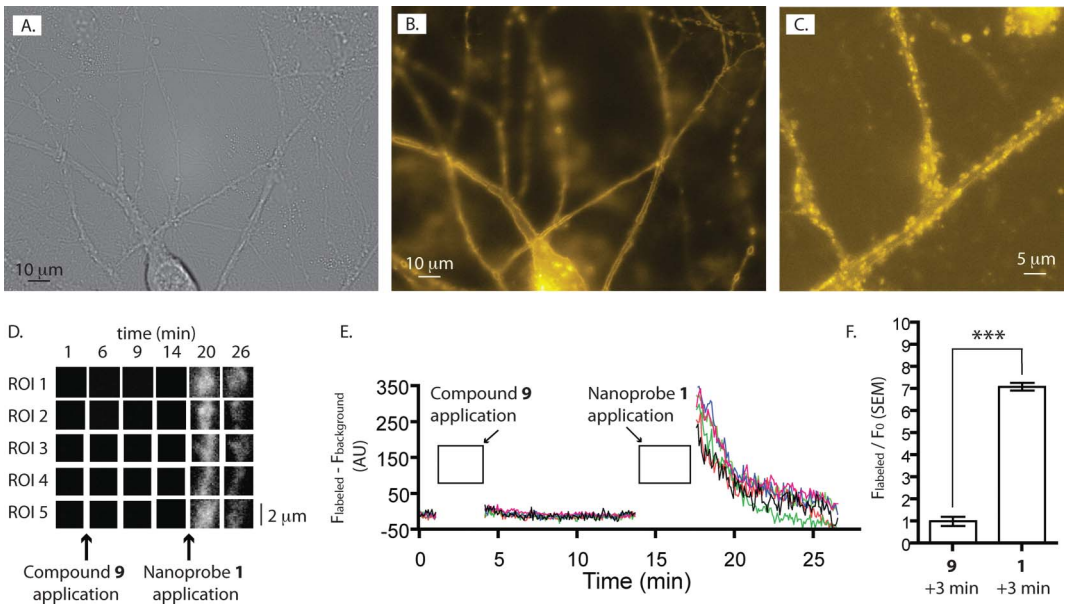

Fig. 3 Nanoprobe **1** labels native neurons. A) Transmitted light image of dissociated hippocampal cultured cells 24 days after plating. Scale bar is 10 μm. B) Fluorescent image of same region 30 s after incubation and wash off of nanoprobe **1**. Scale bar is 10 μm. C) Magnified fluorescent image of a region of hippocampal neurons that was treated with nanoprobe **1** and then washed for 5 min with extracellular buffer. Scale bar is 5 μm. D) Background-subtracted fluorescence signal measured over time of representative synaptic spines. Five representative ROI-focused time points are presented demonstrating little to no fluorescence after application of compound **9**, but lasting fluorescence after application of nanoprobe **1**. Decay in fluorescence between last two time points is a function of photobleaching of the Cy3 chromophore. Scale bar is 2 μm. E) Quantitative analysis of labeling. ROI regions were placed over putative spines then followed before and after addition of compound **9** or nanoprobe **1**. F) Comparison of normalized fluorescence at putative spines (n = 131, images = 7) at two time points. First bar represents the fluorescence at spines 3 min after washout of compound **9** and second bar represents the fluorescence at spines 3 min after washout of nanoprobe **1**. Fluorescence from compound **9** after 3 min of perfusion is significantly greater than the lasting fluorescence from treatment with nanoprobe **1** and 3 min of washing (***$P < 0.00001$, paired t-test).

In the near future, this molecule will be used in orthogonal labeling studies to address the open question of the role of calcium-permeable non-NMDA glutamate receptors in long-term potentiation.

Experimental section

General information

All reagents, biological and chemical, were purchased through Fisher Scientific (Fair Lawn, NJ, USA). All reactions involving air- and moisture-sensitive reagents were performed under an argon atmosphere using syringe-septum cap techniques. DMF and CH_2Cl_2 were dried by storing over molecular sieves (4 A°). Analytical thin-layer chromatography (TLC) was carried out using Merck Silica gel 60 F254 aluminum sheets. Compounds were detected as single spots on TLC plates and visualized using UV light (254 or 366 nm) and $KMnO_4$ or ninhydrin. Merck silica gel (35–70 mesh) was used for flash chromatography. ^{1}H NMR spectra were recorded on a 400 MHz Bruker NMR spectrometer using the residual proton resonance of the solvent as the standard. Chemical shifts are reported in parts per million (ppm). When peak multiplicities are given, the following abbreviations are used: s, singlet; bs, broad singlet; d, doublet; t, triplet; q, quartet; m, multiplet. ^{13}C NMR spectra were proton decoupled and recorded on a 100 MHz spectrometer using carbon signal of the deuterated solvent as the internal standard. Mass spectra were measured either on a Waters ZQ device for LRMS, at the UMass Mass Spectrometry facility for HRMS, or using the Notre Dame Mass Spectrometry and Proteomics Facility. The Nanoprobe excitation and emission wavelengths were measured by Photon Technology International Inc. Instrument, PTI Felix32 software, 3.5 mL volume, 10 mm path length cuvette.

2-Amino-5-(4-methoxycarbonylmethoxy-7-nitro-2,3-dihydro-indol-1-yl)-5-oxo-pentanoic acid *tert*-butyl ester (3). Compound **2** (1.80 g, 3.40 mmol) was dissolved in dry CH_2Cl_2 (4.9 mL) and treated with dichloroacetic acid (4.9 mL, 60.45 mmol) and stirred at room temperature. After 21 h, the reaction mixture was diluted with CH_2Cl_2 (100 mL), washed with sat. aq. $NaHCO_3$ (1 × 80 mL), dried with anhydrous $MgSO_4$, filtered, and evaporated to afford compound **3** as yellow oil (1.34 g, 91%) which was used in the next step without further purification. R_f 0.2 (EtOAc/MeOH 95 : 5). IR (NaCl thin film) ν_{max}: 3351, 2917, 1736, 1676, 1618, 1522, 1283, 1221, 1102 cm^{-1}. ^{1}H-NMR in CD_3OD (400 MHz): δ = 7.71 (d, 1H, J = 9.00 Hz) 6.75 (d, 1H, J = 9.08 Hz), 4.90 (s, 2H), 4.31–4.33(m, 2H), 3.71 (s, 3H), 3.58 (t, 1H, J = 8.27 Hz), 3.16–3.20 (m, 2H), 2.68–2.72 (m, 2H), 2.09–2.13 (m, 1H), 1.97–2.01 (m, 1H), 1.48 (s, 9H). LCMS (ESI-TOF) Calc for $C_{20}H_{28}N_3O_8$ [M+1]: 438.1871. Found: 438.1901.

(S)-*tert*-butyl-2-(6-acrylamidohexanamido)-5-(4-(2-methoxy-2-oxoethoxy)-7-nitroindolin-1-yl)-5-oxopentanoate (5). Functionalized acrylamide **4** (0.465 g, 2.51 mmol) was dissolved in dry DMF (5 mL) and activated with HATU (0.924 g, 2.43 mmol), HOAt (0.376 g, 2.76 mmol), and collidine (3.04 g, 25.0 mmol) at room temperature. After 2 h, pre-dissolved compound **3** (1.10 g,

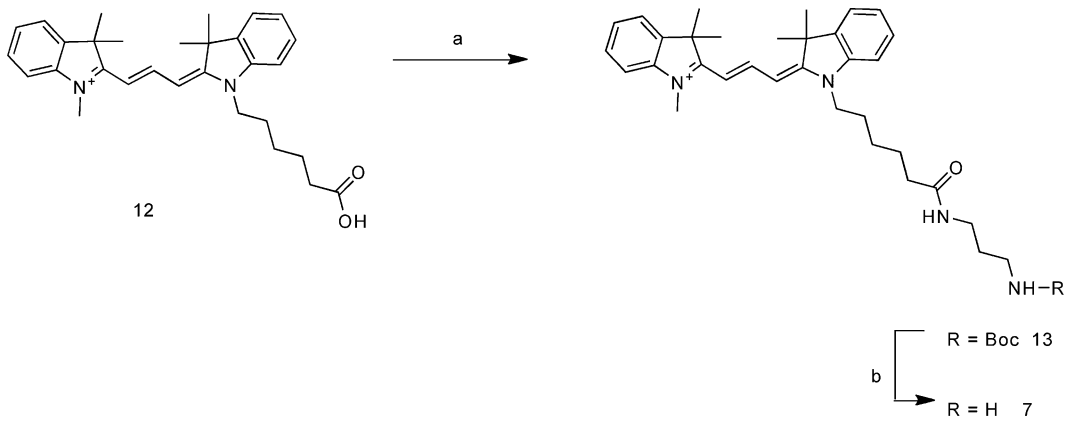

Reagents and conditions : a) Mono-Boc protected propylamine, EDC, HOBt, DIPEA, DMF, rt, 12 h 70%; b) 5% TFA in CH_2Cl_2, rt, 3 h, 90%.

Scheme 2

2.51 mmol) in DMF (2 mL) was added to the reaction mixture and stirring continued for 21 h. The organic solvent was removed under vacuum and the crude liquid was dissolved in EtOAc (100 mL), washed with 1 M citric acid (1 × 80 mL), and sat. aq $NaHCO_3$ (1 × 80 mL), and brine (1 × 80 mL). The solvent was dried with anhydrous Na_2SO_4, filtered, and evaporated. The crude solid was purified by silica-gel chromatography (EtOAc/MeOH gradient 100/0 to 98/2) to afford a light yellow foam **5** (0.760 g, 50%). R_f 0.3 (EtOAc/MeOH 95 : 5). IR (NaCl thin film) ν_{max}: 3362, 2917, 1731, 1662, 1610, 1519, 1283, 1220, 1152, 1102 cm^{-1}. ^{1}H-NMR in $CDCl_3$ (400 MHz): δ = 7.68 (d, 1H, J = 9.01 Hz), 6.50 (d, 1H, J = 9.05 Hz), 6.26 (d, 1H, J = 16.8 Hz), 6.10 (dd, 1H, J = 6.74 Hz, J 2 = 10.2 Hz), 5.59 (d, 1H, J = 10.2 Hz), 4.74 (s, 2H), 4.49–4.43 (m, 1H), 4.23 (t, 2H, J = 8.18 Hz), 3.81 (s, 3H), 3.33–3.29 (q, 2H), 3.18 (t, 2H, J = 8.00 Hz), 2.66–2.52 (m, 2H), 2.28–2.10 (m, 4H), 1.68–1.60 (m, 2H), 1.56–1.49 (m, 2H), 1.45 (s, 9H), 1.40–1.29 (m, 2H). HRMS (ESI-TOF) Calc for $C_{29}H_{41}N_4O_{10}$ [M+1]: 605.2849. Found: 605.2817.

2-(6-Acryloylamino-hexanoylamino)-5-(4-methoxycarbonyl-methoxy-7-nitro-2,3-dihydro-indol-1-yl)-5-oxo-pentanoic acid (6). Compound **5** (730 mg, 1.20 mmol) was treated with 10% TFA in dry CH_2Cl_2 (50 mL) for 12 h at room temperature. When consumption of the starting material was confirmed by TLC (CH_2Cl_2/MeOH 90 : 10), the solvent was evaporated to afford a light yellow foam **6** (640 mg, 96%). R_f 0.3 (CH_2Cl_2/MeOH 85 : 5). IR (NaCl, thin film) ν_{max}: 3412, 2928, 1710, 1654, 1525, 1432, 1393, 1286, 1226, 801 cm^{-1}. ^{1}H-NMR in $CDCl_3$ (400 MHz): δ = 7.62 (d, 1H, J = 9.01 Hz), 6.86 (bs, 1H), 6.60 (bs, 1H), 6.48 (d, 1H, J = 9.05 Hz), 6.06–6.21 (m, 2H), 5.50 (dd, 1H, $J1$ = 7.25 Hz, $J2$ = 2.56 Hz), 4.69 (s, 2H), 4.42–4.47 (m, 1H), 4.18 (t, 2H, J = 6.53 Hz), 3.73 (s, 3H), 3.19–3.24 (q, 2H), 3.11 (t, 2H, J = 7.63 Hz), 2.54–2.66 (m, 2H), 2.20–2.23 (m, 4H), 1.53–1.62 (m, 2H), 1.42–1.49 (m, 2H), 1.29–1.36 (m, 2H). HRMS (ESI-TOF) Calc for $C_{25}H_{33}N_4O_{10}$ [M+1] m/z: 549.2181, Found: 549.2191.

2-(3-{1-[5-(3-Amino-propylcarbamoyl)-pentyl]-3,3-dimethyl-1,3-dihydro-indol-2-ylidene}-propenyl)-1,3,3-trimethyl-3*H*-indolium (7). Compound **12** (580 mg, 1.26 mmol)[40] was dissolved in dry DMF (5 mL) and treated with EDC HCl (274 mg, 1.39 mmol), HOBt (166 mg, 1.23 mmol), and DIPEA (491 mg, 3.80 mmol) (Scheme 2). The reaction mixture was stirred for 30 min at room temperature. Mono-boc-protected propyldiamine was added to the reaction mixture and stirring was continued for 12 h. The DMF was removed under vacuum and the residue dissolved in $CHCl_3$ (50 mL). The solvent was washed with sat. aq. $NaHCO_3$ (1 × 50 mL), 1 M citric acid (1 × 50 mL), and brine (1 × 50 mL), and then dried with anhydrous $MgSO_4$, filtered, and evaporated. The residue was purified by silica-gel chromatography ($CHCl_3$/MeOH gradient 100/0 to 90/10) to afford the compound **13** as a pink solid (544 mg, 70%). R_f 0.4 ($CHCl_3$/MeOH 85 : 15). IR (NaCl, thin film) ν_{max}: 3406, 2967, 1695, 1632, 1558, 1451, 1418, 1369, 1207, 1152, 919 cm^{-1}. ^{1}H-NMR in $CDCl_3$ (400 MHz): δ = 8.45 (t, 1H, J = 13.4 Hz), 7.34–7.42 (m, 6H), 7.23–7.28 (m, 2H), 7.09–7.12 (m. 2H), 5.48 (bs, 1H), 4.13 (t, 2H, J = 7.58 Hz), 3.83 (s, 3H), 3.28–3.32 (m, 2H), 3.10–3.14 (m, 2H), 2.42 (t, 2H, J = 7.07 Hz), 1.79–1.85 (m, 2H), 1.71 (s, 12H), 1.49–1.69 (m, 4H), 1.38 (s, 9H). HRMS (ESI-TOF) Calc for $C_{38}H_{53}N_4O_3^+$ [M^+]: 613.4125, Found: 613.4112.

Compound **13** was then treated with 5% TFA in CH_2Cl_2 (10 mL) at room temperature and stirring was continued for 16 h. Reaction progress was monitored by TLC and the solvent was removed to afford compound **7** (409 mg, 90%). R_f 0.1 ($CHCl_3$/MeOH 85 : 5). IR (NaCl, thin film) ν_{max}: 3428, 2934, 1679, 1640, 1561, 1456, 1407, 1201, 1119, 930 cm^{-1}. ^{1}H-NMR in $CDCl_3$ (400 MHz): δ = 8.41 (t, 1H, J = 13.4 Hz), 7.36–7.44 (m, 3H), 7.26–7.30 (m, 3H), 7.14–7.16 (m. 2H), 6.38–6.41 (dd, 2H, $J1$ = 13.39, $J2$ = 16.17 Hz), 5.48 (bs, 1H), 4.02 (t, 2H, J = 7.33 Hz), 3.63 (s, 3H), 3.39–3.42 (m, 2H), 3.04–3.08 (m, 2H), 2.38 (t, 2H, J = 7.07 Hz), 1.95–1.99 (m, 2H), 1.77–1.88 (m, 2H), 1.72–1.71 (m, 12H), 1.43–1.62 (m, 4H). HRMS (ESI-TOF) Calc for $C_{33}H_{45}N_4O^+$ [M^+]: 513.3623, Found: 513.3588.

2-{3-[1-(5-{3-[2-(6-Acryloylamino-hexanoylamino)-5-(4-carboxymethoxy-7-nitro-2,3-dihydro-indol-1-yl)-5-oxo-pentanoylamino]-propylcarbamoyl}-pentyl)-3,3-dimethyl-1,3-dihydro-indol-2-ylidene]-propenyl}-1,3,3-trimethyl-3*H*-indolium (8). Compound **6** (250 mg, 0.454 mmol) was treated with HATU (190 mg, 0.501 mmol), HOAt (62 mg, 0.442 mmol), and collidine (551 mg, 4.5 mmol) in DMF (2.5 mL) at room temperature for 4 h. Compound **7** (260 mg, 0.5 mmol) was then added to the reaction

mixture and stirring was continued for 24 h. The DMF was removed under reduced pressure, the residue dissolved in $CHCl_3$ (50 mL), washed with 1 M citric acid (1 × 50 mL), sat. aq. $NaHCO_3$ (1 × 50 mL), and brine (1 × 50 mL). The solvent was dried with anhydrous $MgSO_4$, filtered, and evaporated. The residue was then purified by silica-gel column chromatography ($CHCl_3$/MeOH gradient 100/0 to 90/10) to afford the pink solid **8** (220 mg, 58%). R_f 0.3 ($CHCl_3$/MeOH 85 : 15). IR (NaCl, thin film) ν_{max}: 3406, 2917, 1659, 1555, 1459, 1415, 1369, 1223, 1105, 839 cm^{-1}. ^{1}H-NMR in CD_3OD (400 MHz): δ = 8.53 (t, 1H, J = 13.39 Hz), 7.63–7.70 (m, 3H), 7.53 (d, 2H, J = 7.58 Hz), 7.43 (t, 2H, J = 7.83 Hz), 7.27–7.34 (m, 4H), 6.74 (t, 1H, J = 7.83 Hz), 6.44 (d, 2H, J = 13.39 Hz), 6.18–6.21 (m, 2H), 5.60–5. 64 (m, 1H), 4.90 (s, 1H), 4.88 (s, 2H), 4.25–4.33 (m, 4H), 4.14 (t, 2H, J = 7.33 Hz), 3.77 (s, 3H), 3.13–3.25 (m, 8H), 2.61–2.66 (m, 2H), 2.20–2.31 (m, 6H), 1.96–2.16 (m, 2H), 1.80–1.88 (m, 2H), 1.75 (s, 12H), 1.58–1.72 (m, 4H), 1.44–1.56 (m, 2H), 1.29–1.40 (m, 2H). ^{13}C-NMR in CD_3OD (100 MHz): δ = 175.21, 174.88, 174.51, 172.59, 171.41, 171.36, 169.0, 166.63, 157.3, 150.69, 142.69, 141.98, 140.79, 136.29, 135.58, 130.73, 128.6, 128.52, 125.3, 125.0, 124.58, 123.93, 122.11, 121.95, 111.06, 110.87, 107.57, 64.83, 53.15, 51.37, 49.91, 49.21, 49.16, 43.65, 38.85, 36.44, 36.35, 36.22, 35.35, 35.25, 31.42, 30.39, 28.74, 28.62, 26.94, 26.84, 26.78, 26.5, 26.17, 25.82, 25.15, 24.98, 21.19. HRMS (ESI-TOF) Calc for $C_{58}H_{75}N_8O_{10}^+$ [M$^+$]: 1043.5632, Found: 1043.5601.

2-{3-[1-(5-{3-[2-(6-Acryloylamino-hexanoylamino)-5-(4-carboxymethoxy-7-nitro-2,3-dihydro-indol-1-yl)-5-oxo-pentanoylamino]-propylcarbamoyl}-pentyl)-3,3-dimethyl-1,3-dihydro-indol-2-ylidene]-propenyl}-1,3,3-trimethyl-3*H*-indolium (Compound 9). Compound **8** (110 mg, 0.108 mmol) was dissolved in MeOH (2 mL) and treated with aq. 1 N NaOH (150 µL, 0.15 mmol) at room temperature for 2 h. When consumption of the starting material was confirmed by TLC (CH_2Cl_2/MeOH 90 : 10) the reaction mixture was neutralized with 1 M citric acid (150 µl) and concentrated under vacuum. The residue was diluted with water, acidified to pH 2 with 1 M citric acid and washed with EtOAc. The combined organic phases were washed with brine, dried with anhydrous $MgSO_4$, filtered, and evaporated to afford compound **9** as pink colored foam (100 mg, 97%). R_f 0.2 ($CHCl_3$/MeOH 50 : 50). IR (NaCl, thin film) ν_{max}: 3274, 2928, 1651, 1610, 1555, 1454, 1407, 1223, 1113 cm^{-1}. ^{1}H-NMR in CD_3OD (400 MHz): δ = 8.44 (t, 1H, J = 13.39 Hz), 7.56 (d, 1H, J = 8.84 Hz), 7.36–7.43 (m, 4H), 7.21–7.27 (m, 4H), 6.58 (d, 1H, J = 9.09 Hz), 6.30–6.35 (dd, 2H, $J1$ = 13.39, $J2$ = 6.06 Hz), 6.14–6.15 (m, 2H), 5.53–5.56 (dd, 1H, $J1$ = 7.33 Hz, $J2$ = 2.53 Hz), 4.51 (s, 1H), 4.25–4.28 (m, 1H), 4.20 (t, 2H, J = 7.85 Hz), 4.05 (t, 2H, J = 7.33 Hz), 3.61 (s, 3H), 3.13–3.19 (m, 10H), 2.49–2.64 (m, 2H), 2.16–2.24 (m, 4H), 1.91–2.01 (m, 2H), 1.76–1.84 (m, 2H), 1.71 (s, 12H), 1.54–1.68 (m, 6H), 1.41–1.52 (m, 4H), 1.26–1.35 (m, 4H). ^{13}C-NMR in CD_3OD (100 MHz): δ = 176.2, 176.0, 175.6, 173.7, 172.5, 167.9, 159.5, 151.8, 143.7, 143.0, 141.8, 141.6, 136.2, 132.0, 130.0, 126.8, 124.9, 123.4, 123.2, 112.3, 112.1, 108.9, 103.8, 103.6, 54.4, 51.1, 50.5, 50.4, 45.1, 40.2, 37.6, 37.5, 37.4, 36.8, 36.7, 32.9, 32.0, 30.7, 29.8, 28.7, 28.6, 27.5, 27.3, 26.4, 26.2, HRMS (ESI-TOF) Calc for $C_{57}H_{73}N_8O_{10}^+$ [M$^+$]: 1029.5467, Found: 1029.5444.

***N*-[3-(*tert*-Butoxycarbonyl-{4-[*tert*-butoxycarbonyl-(3-*tert*-butoxycarbonylamino-propyl)-amino]-butyl}-amino)-propyl]-succinamic acid methyl ester (16).** Ester **15** (0.531 g, 4.02 mmol) was dissolved in dry CH_2Cl_2 (50 mL) and treated with EDC.HCl (1.0 g, 5.24 mmol), HOBt (0.652 g, 4.8 mmol) and triethylamine (0.4 g, 4.02 mmol) at –20 °C and was stirred for 4 h. The solution of tri-boc spermine **14** (2.0 g, 4.02 mmol) in CH_2Cl_2 (20 mL) was added over a period of 15 min to the reaction mixture and stirring continued for 16 h at room temperature. The reaction mixture was diluted with CH_2Cl_2 (20 mL) and washed with sat. aq. $NaHCO_3$ (1 × 20 mL), 1 M citric acid (1 × 20 mL), and brine (1 × 20 mL). The organic layer was dried with anhydrous $MgSO_4$, filtered and evaporated. The crude product was purified by silica-gel chromatography (EtOAc/MeOH/NH_3 gradient 95/5/0.01 to 80/20/1) to afford the title compound **16** (2.2 g, 91%) as colorless liquid (Scheme 3). R_f 0.4 (EtOAc/MeOH/NH_3 95 : 5 : 0.01). IR (NaCl, thin film) ν_{max}: 3351, 2934, 2972, 1690, 1530, 1412, 1366, 1248, 1160 cm^{-1}. ^{1}H-NMR in $CDCl_3$ (400 MHz): 3.71 (s, 3H), 3.15–3.30 (m, 12H), 2.73 (t, 2H, J = 5.65 Hz), 2.52 (t, 2H, J = 5.69 Hz), 1.72–1.63 (m, 4H), 1.46–1.48 (m, 31H). HRMS (ESI-TOF): Calc for $C_{30}H_{57}N_4O_9$ [M+1]: 617.4154. Found: 617.4154.

***N*-[3-(*tert*-Butoxycarbonyl-{4-[*tert*-butoxycarbonyl-(3-*tert*-butoxycarbonylamino-propyl)-amino]-butyl}-amino)-propyl]-succinamic acid (17).** Compound **16** (1.1 g, 1.7 mmol) was dissolved in MeOH (30 mL), treated with aq. 1 N NaOH (3 mL) and stirred at room temperature for 12 h. The MeOH was removed, water (5 mL) was added to the reaction mixture which was then acidified to pH 2 with 1 M citric acid and extracted with EtOAc (3 × 50 mL). The combined organic layers were dried with anhydrous Na_2SO_4 and evaporated to afford the title compound **17** (0.98 g, 92%) as a white foam. R_f 0.2 (EtOAc/MeOH/NH_3 95 : 5 : 0.01). IR (NaCl, thin film) ν_{max}: 3362, 2956, 1692, 1659, 1476, 1421, 1245, 1176 cm^{-1}. ^{1}H-NMR in $CDCl_3$ (400 MHz): 3.08–3.20 (m, 12H), 2.63 (t, 2H, J = 6.02 Hz), 2.48 (bs, 2H), 1.64 (m, 4H), 1.41–1.43 (m, 31H). HRMS (ESI-TOF): Calc for $C_{29}H_{55}N_4O_9$ [M+1]: 603.3964. Found: 603.3982.

(3-*tert*-Butoxycarbonylamino-propyl)-{4-[*tert*-butoxycarbonyl-(3-{3-[4-(9*H*-fluoren-9-yl-methoxycarbonylamino)-butylcarbamoyl]-propionylamino}-propyl)-amino]-butyl}-carbamic acid *tert*-butyl ester (19). The compound **17** (490 mg, 0.815 mmol) was dissolved in a 50/50 mixture of CH_2Cl_2 : DMF (10 mL) and treated with HOBt (132 mg, 0.97 mmol), HBTU (402 mg, 1.05 mmol), and DIPEA (210 mg, 1.62 mmol). The reaction mixture was stirred for 1 h at room temperature. The Fmoc -protected 1,4-diaminobutane **18** (505 mg, 1.65 mmol) was added to the reaction mixture and stirring continued for 12 h at room temperature. The organic solvent was evaporated and dissolved in EtOAc (50 mL), washed with sat. aq. $NaHCO_3$ (1 × 40 mL) followed by 1 M citric acid (1 × 40 mL) and brine (1 × 40 mL). The organic extracts were dried with anhydrous Na_2SO_4 and evaporated. The crude product was purified by using silica gel chromatography (CH_2Cl_2/MeOH/NH_3 gradient 99/1/0 to 95/5/0.01) to afford the pure compound **19** as a white solid (395 mg, 57%). R_f 0.4 (CH_2Cl_2/MeOH/NH_3 95 : 5 : 0.01). IR (NaCl, thin film) ν_{max}: 3423, 3314, 2917, 1690, 1665, 1530, 1253, 1160, 845 cm^{-1}. ^{1}H-NMR in CD_3OD (400 MHz): δ = 7.77 (d, 2H, J = 9.12 Hz), 7.62 (d, 2H, J = 9.15 Hz), 7.36 (t, 2H, J = 8.25 Hz), 7.28 (t, 2H, J = 8.57 Hz), 4.31 (d, 2H, J = 8.64 Hz), 4.17 (t, 1H, J = 5.9 Hz), 3.32 (bs, 6H), 3.09–3.28 (m, 12H), 3.00 (t, 2H, J = 6.98 Hz), 2.45 (bs, 4H), 1.66 (bs, 4H), 1.42 (bs, 8H),

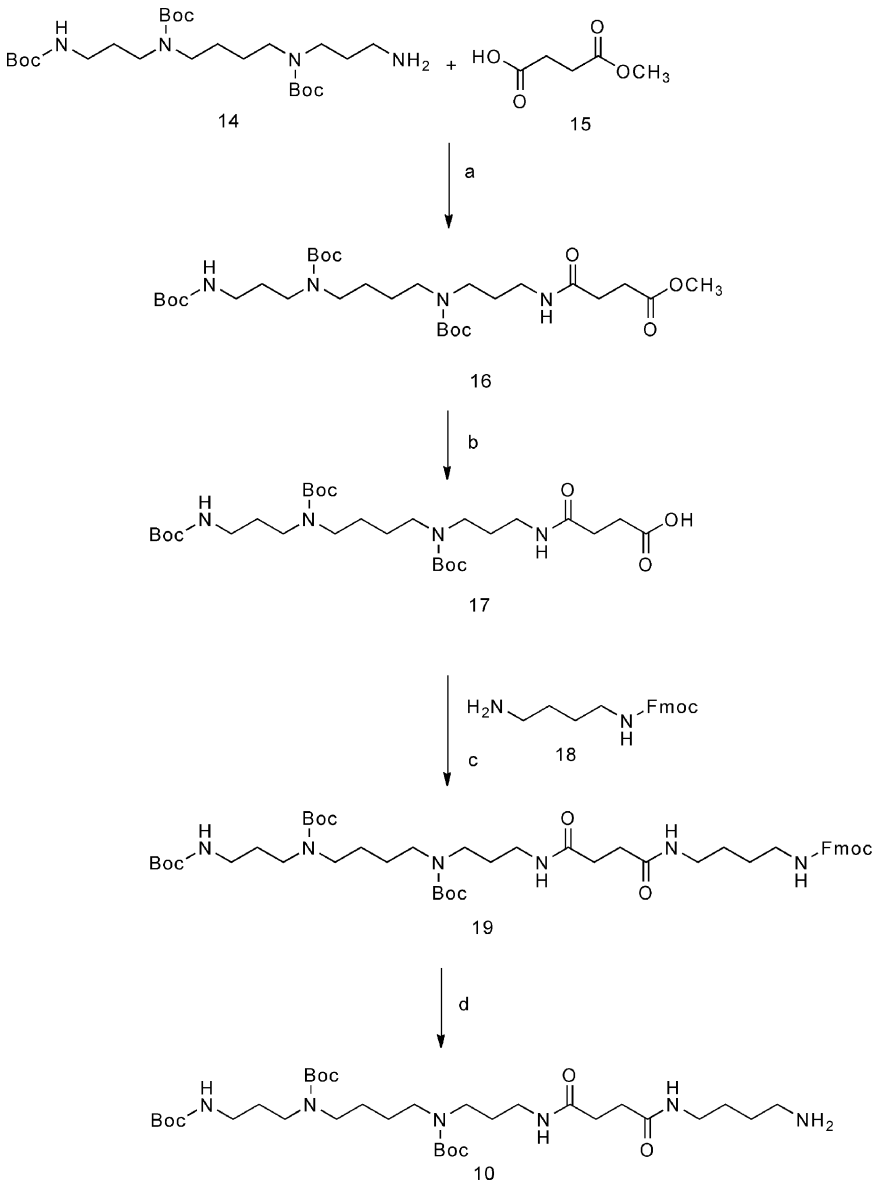

Scheme 3

1.40 (s, 27H). LCMS (ESI) Calc for $C_{48}H_{75}N_6O_{10}$ [M+1]: 895.5545. Found: 895.5539.

(3-{[4-({3-[3-(4-Amino-butylcarbamoyl)-propionylamino]-propyl}-*tert*-butoxycarbonyl-amino)-butyl]-*tert*-butoxycarbonyl-amino}-propyl)-carbamicacid *tert*-butyl ester (10). Compound **19** (225 mg, 0.245 mmol) was treated with 50% piperidine in DMF (1 mL) at room temperature for 30 min. The solvent was removed under reduced pressure and the crude product was purified by silica-gel chromatography (CH_2Cl_2/MeOH/NH_3 gradient 80/10/0.1 to 50/10/1) to afford a colorless liquid compound **10** (100 mg, 59%). R_f 0.4 (CH_2Cl_2/MeOH/NH_3 50 : 10 : 1). IR (NaCl, thin film) ν_{max}: 3324, 2972, 2923, 1668, 1544, 1473, 1415, 1363, 1248, 1166 cm^{-1}. ^{1}H-NMR in CD_3OD (400 MHz): δ = 3.34 (s, 2H), 3.14–3.22 (m, 12H), 3.03 (t, 2H, J = 7.8 Hz), 2.66 (t, 2H, J = 7.69 Hz), 2.46 (s, 4H), 1.70 (bs, 4H), 1.46 (bs, 8H), 1.43 (s, 27H). HRMS (ESI-TOF) Calc for $C_{33}H_{65}N_6O_8$ [M+1]: 673.4885. Found: 673.4858.

Compound 11. Compound **9** (10 mg, 0.012 mmol) was dissolved in dry 4 : 1 CH_3CN : DMF (1 mL) and treated with compound **10** (8.1 mg, 0.012 mmol) and EDC HCl (3.5 mg, 0.018 mmol). The mixture was stirred at room temperature under nitrogen for 48 h and then evaporated. The residue was dissolved in EtOAc (5 mL) and washed with 0.5 M aq. HCl (1 × 5 mL), sat. aq. $NaHCO_3$ (1 × 5 mL), and then brine (1 × 5 mL), dried with anhydrous Na_2SO_4, filtered and evaporated. The crude product was purified by silica-gel column chromatography ($CHCl_3$/MeOH gradient 95/5 to 80/10) to afford the title compound **11** (10 mg, 56%). R_f 0.6 ($CHCl_3$/MeOH 87 : 13). IR (NaCl, thin film) ν_{max}:

3417, 3313, 2928, 1659, 1555, 1459, 1412, 1360, 1275, 1229, 1157, 921 cm^{-1}. ^{1}H-NMR in CD_3OD (400 MHz): δ = 8.54 (t, 1H, *J* = 13.64 Hz), 7.69 (d, 1H, *J* = 9.09 Hz), 7.53 (d, 2H, *J* = 7.58 Hz), 7.28–7.46 (m, 6H), 6.75 (d, 1H, *J* = 9.09 Hz), 6.46 (dd, 2H, *J1* = 2.78 Hz, *J2* = 10.39 Hz), 6.18–6.21 (m, 2H), 5.56 (dd, 1H, *J1* = 3.58 Hz, *J2* = 5.38 Hz), 4.67 (s, 2H), 4.27–4.33 (m, 3H), 4.17 (t, 2H, *J* = 7.53 Hz), 3.68 (s, 3H), 3.13–3.27 (m, 19H), 3.02 (t, 2H, *J* = 6.57), 2.59–2.69 (m, 2H), 2.45 (bs, 4H), 2.11–2.31 (m, 6H), 1.81–2.18 (m, 4H), 1.80–1.88 (m, 4H), 1.76 (s, 12H), 1.61–1.72 (m, 6H), 1.45–1.46 (m, 29H), 1.29–1.40 (m, 4H). ^{13}C-NMR in CD_3OD (100 MHz): δ = 176.5, 176.29, 175.97, 175.87, 174.53, 174.04, 172.76, 169.97, 158.56, 152.10, 144.10, 143.40, 142.19, 142.10, 137.77, 137.16, 132.17, 130.06, 129.97, 126.76, 126.49, 126.10, 125.95, 125.53, 123.55, 123.39, 112.50, 112.31, 109.03, 103.83, 103.69, 80.96, 68.59, 54.82, 54.56, 51.36, 50.67, 50.61, 49.89, 49.84, 49.72, 40.26, 40.0, 39.87, 37.76, 36.75, 36.68, 32.88, 31.82, 30.79, 30.79, 30.17, 30.07, 28.83, 28.79, 28.37, 28.27, 28.19, 27.76, 27.71, 27.60, 27.32, 27.29, 26.56, 26.42. HRMS (FAB) Calc for $C_{90}H_{135}N_{14}O_{17}^+$ [M^+]: 1684.0124. Found: 1684.0130.

Nanoprobe 1. Compound **11** (8.5 mg, 0.005 mmol) was treated with 20% TFA in dry CH_2Cl_2 (1 mL) at 0 °C to room temperature for 3 h. When consumption of the starting material was confirmed by TLC (CH_2Cl_2/MeOH/NH_3 80 : 20 : 1) the organic solvent was evaporated to afford the title compound nanoprobe **1** as dark pink solid (7.8 mg, 98%). R_f 0.1 ($CHCl_3$/MeOH 83 : 17). IR (NaCl, thin film) ν_{max}: 3417, 3313, 2928, 1659, 1555, 1459, 1412, 1360, 1275, 1229, 1157, 921 cm^{-1}. λ_{max}, excitation: 534 nm, emission: 566 nm. ^{1}H-NMR in CD_3OD (400 MHz): δ = 8.54 (t, 1H, *J* = 13.39 Hz), 7.70 (d, 1H, *J* = 9.09 Hz), 7.54 (d, 2H, *J* = 7.58 Hz), 7.42–7.47 (m, 2H), 7.29–7.36 (m, 4H), 6.76 (d, 1H, *J* = 9.09 Hz), 6.42 (d, 2H, *J* = 13.39 Hz), 6.18–6.21 (m, 2H), 5.60–5.63 (dd, 1H, *J1* = 8.84 Hz, *J2* = 5.56 Hz), 4.94 (s, 1H), 4.69 (s, 2H), 4.27–4.32 (m, 2H), 4.17 (t, 2H, *J* = 7.33 Hz), 3.68 (s, 3H), 3.02–3.35 (m, 24H), 2.60–2.70 (m, 2H), 2.44–2.54 (m, 4H), 2.28 (t, 2H, *J* = 7.33 Hz), 2.22 (t, 2H, *J* = 7.33 Hz), 2.05–2.15 (m, 2H), 1.79–1.92 (m, 4H), 1.76 (s, 12H), 1.60–1.74 (m, 6H), 1.45–1.58 (m, 8H), 1.31–1.41 (m, 2H). ^{13}C-NMR in CD_3OD (100 MHz): δ = 176.67, 176.34, 176.15, 175.97, 175.90, 174.42, 174.06, 172.78, 170.06, 168.04, 165.02, 160.77, 158.59, 152.10, 144.08, 143.39, 142.18, 142.08, 137.74, 137.12, 132.13, 130.02, 129.96, 126.75, 126.48, 126.09, 125.54, 123.54, 123.38, 112.46, 112.29, 109.01, 103.80, 103.65, 68.58, 51.36, 50.66, 50.62, 49.85, 49.83, 49.71, 48.13, 46.16, 45.91, 45.06, 40.24, 39.98, 39.81, 37.85, 37.85, 37.76, 37.62, 36.74, 36.68, 32.79, 31.98, 31.82, 30.82, 28.33, 28.27, 28.17, 27.75, 27.58, 27.34, 27.26, 26.59, 26.40, 25.21, 24.33, 24.28. HRMS (FAB) Calc for $C_{75}H_{111}N_{14}O_{11}^+$ [M^+]: 1384.7935. Found: 1384.8707.

HEK293T cell culture

Cells were cultured on glass in 10% FBS in DMEM media to 70% confluency. Cells were grown in 6% CO_2 at 37 °C and were transfected with a bicistronic vector GluA1(L497Y)-pIRES2-eGFP[45] using LipoD293 (SignaGen Laboratories, Gaithersburg, MD, USA) 1–3 days before electrophysiological recordings.

Patch clamp electrophysiology

Patch pipettes (2–6 MΩ) were filled with 10 mM NaCl, 135 mM K-gluconate, 10 mM HEPES, 2 mM $MgCl_2$, 2 mM Mg-ATP, and 1 mM EGTA at pH 7.4. Extracellular recording buffer contained 138 mM NaCl, 1.5 mM KCl, 1.2 mM $MgCl_2$, 5 mM HEPES, 2.5 mM $CaCl_2$ and 14 mM glucose at pH 7.4. The concentration of DMSO in the bath did not exceed 0.1%. After washout of residual media, whole cell patch configuration was established. To determine use-dependency of nanoprobe **1**, voltage-clamp configuration (–70 mV) was used to measure glutamate-evoked current from applied 20 μM glutamate before and after treatment with either a solution of 20 μM glutamate and 1 μM nanoprobe **1**, or with a solution of 1 μM nanoprobe **1** alone. Pulse protocols and measurements were carried out with pCLAMP 9.0 software, a DigiData 1200 series interface, and an AxoPatch 200A amplifier (Molecular Devices, Sunnyvale, CA, USA). Samples were acquired at 10 kHz and the data filtered at 1 kHz.

Normalized glutamate-evoked currents were determined by the average of three 1 s pulses of 20 μM glutamate at the beginning of each recording delivered 1 min apart to minimize desensitization. Glutamate test pulses were followed by a 1 min application of a solution of 20 μM glutamate and 1 μM nanoprobe **1**, with extracellular perfusion turned off. After incubation, perfusion was reinstated and washing was performed for 1 min. While maintaining continuous perfusion, a 1 s challenge pulse of 20 μM glutamate was applied. This was followed 15 s later by another 1 s pulse of 20 μM glutamate, this time in combination with a 15 s exposure to 380 nm radiation applied using light filtered through a 380/30 nm filter (Chroma Technology, Bellows Falls, VT, USA) from a Prior 200 illuminator (Rockland, MA, USA). After photolytic release of the ligand, glutamate-evoked current was measured by three 1 s pulses of 20 μM glutamate spaced 1 min apart.

To measure the use-dependent nature of nanoprobe **1**, normalized current was measured with three 1 s 20 μM glutamate pulses spaced 1 min apart and then cells were incubated with 1 μM nanoprobe **1** alone in a sequence identical to the above experiment for 1 min, followed by 1 min of perfusion. While maintaining continual perfusion, a 1 s challenge pulse of 20 μM glutamate was applied, followed 15 s later by another 1 s pulse of 20 μM glutamate in combination with 15 s of UV radiation to measure UV-induced glutamate-evoked current recovery.

Dissociated hippocampal cell culture

Primary dissociated hippocampal cultures were prepared from embryonic day E18-19 Sprague–Dawley rat embryos and were cultured on polylysine-coated coverglass (25.5 mm, 1.0 size) in serum-containing medium identical to previous reports.[46] Cells were grown in 5% CO_2 at 37 °C. All animal care and experimental protocols were approved by the Animal Care and Use Committee at University of Massachusetts Amherst, Amherst, MA, USA.

Live cell nanoprobe 1 labeling

Cells were imaged by excitation with light from a Sutter Lambda-LS illuminator (Sutter Instruments, Novato, CA, USA). A Nikon Eclipse Ti series microscope (Nikon Corps Tokyo, Japan) with a CFI Plan Apo VC 60X 1.4 NA oil objective lens (Nikon) was employed for all imaging experiments. The Cy3 filter cube contained a 540/30 excitation filter (Omega Optical Cor., Brattleboro, VT, USA), a 570DRLP dichroic mirror (Omega), and a 575ALP

emission filter (Omega). Images were acquired using a Hamamatsu ORCA ER camera (Hamamatsu, Hamamatsu City, Japan) and NIS Elements BR 3.1 software (Nikon Corps Melville, NY, USA).

Cells were mounted in a 25 mm perfusion apparatus (ALA M-525, ALA Scientific, Farmingdale, NY USA) and bathed in extracellular solution made from an identical recipe to the electrophysiology extracellular buffer described above. To maintain fresh recording buffer flow, hippocampal cultures were constantly perfused with extracellular buffer using a perfusion device (ALA-VM8, ALA Scientific) at all times except for the nanoprobe **1** or compound **9** incubations. Fluorescence images were acquired at 20 frames per minute using the Cy3 filter set to capture background and then post-labeled images. Background fluorescence was measured for normally 1 min and then perfusion was stopped leaving minimal buffer on the cells. Next ~200 μL of 750 nM compound **9** was added to the bath and incubated for 2 min. Perfusion was reinstated and imaging was carried out for 10 min at which point background fluorescence was again measured for 1 min and again perfusion was stopped leaving minimal buffer on the cells. Finally, 200 μL of 750 nM nanoprobe **1** was added to the bath and incubated for 2 min. Perfusion was reinstated and imaging was carried out for 10 min.

Image analysis

Images were analyzed using ImageJ (U.S. National Institutes of Health, Bethesda, MD, USA). Fluorescence was quantified using ROI analysis of multiple regions placed over putative synaptic sites and areas of background. The mean fluorescence intensity was background subtracted and normalized to the measured fluorescence at 1 min before the application of compound **9** and the time course was plotted using GraphPad Prism. Seven image series were analyzed and the data combined for a total of 131 ROIs analyzed. GraphPad Prism (La Jolla, CA, USA) was used to plot the data. For data presentation purposes, the contrast of Fig. 3B was enhanced without weighting and all of the raw images that make up Fig. 3E were combined in the montage and then contrast was enhanced so that all images were treated identically. No differential weighting or any other manipulation was used.

Acknowledgements

The GluA1 cDNA was a kind gift from Dr Roger Nicoll (UCSF). The authors would like to thank the Human Frontier Science Program for their support of this work (JJC, IH HFSPO RGY66/2008). RCB was supported by a training grant from the NIH (5 T32 NS007490).

References

1 J. T. Isaac, M. Ashby and C. J. McBain, The role of the GluR2 subunit in AMPA receptor function and synaptic plasticity, *Neuron*, 2007, **54**, 859–871.
2 B. N. G. Giepmans, S. R. Adams, M. H. Ellisman and R. Y. Tsien, Review -The fluorescent toolbox for assessing protein location and function, *Science*, 2006, **312**, 217–224.
3 A. Triller and D. Choquet, New concepts in synaptic biology derived from single-molecule imaging, *Neuron*, 2008, **59**, 359–374.
4 M. Chalfie, Y. Tu, G. Euskirchen, W. W. Ward and D. C. Prasher, Green Fluorescent Protein as a Marker for Gene-Expression, *Science*, 1994, **263**, 802–805.
5 B. A. Griffin, S. R. Adams and R. Y. Tsien, Specific covalent labeling of recombinant protein molecules inside live cells, *Science*, 1998, **281**, 269–272.
6 K. M. Marks, P. D. Braun and G. P. Nolan, A general approach for chemical labeling and rapid, spatially controlled protein inactivation, *Proc. Natl. Acad. Sci. U. S. A.*, 2004, **101**, 9982–9987.
7 C. M. McCann, F. M. Bareyre, J. W. Lichtman and J. R. Sanes, Peptide tags for labeling membrane proteins in live cells with multiple fluorophores, *BioTechniques*, 2005, **38**, 945–952.
8 A. Keppler, S. Gendreizig, T. Gronemeyer, H. Pick, H. Vogel and K. Johnsson, A general method for the covalent labeling of fusion proteins with small molecules in vivo, *Nat. Biotechnol.*, 2002, **21**, 86–89.
9 D. S. Bredt and R. A. Nicoll, AMPA receptor trafficking at excitatory synapses, *Neuron*, 2003, **40**, 361–379.
10 W. Lu, Y. Shi, A. C. Jackson, K. Bjorgan, M. J. During, R. Sprengel, P. H. Seeburg and R. A. Nicoll, Subunit composition of synaptic AMPA receptors revealed by a single-cell genetic approach, *Neuron*, 2009, **62**, 254–268.
11 S. Cull-Candy, L. Kelly and M. Farrant, Regulation of Ca2+-permeable AMPA receptors: synaptic plasticity and beyond, *Curr. Opin. Neurobiol.*, 2006, **16**, 288–297.
12 A. I. Sobolevsky, M. P. Rosconi and E. Gouaux, X-ray structure, symmetry and mechanism of an AMPA-subtype glutamate receptor, *Nature*, 2009, **462**, 745–756.
13 M. Dahan, S. Levi, C. Luccardini, P. Rostaing, B. Riveau and A. Triller, Diffusion dynamics of glycine receptors revealed by single-quantum dot tracking, *Science*, 2003, **302**, 442–445.
14 F. F. Trigo, J. E. Corrie and D. Ogden, Laser photolysis of caged compounds at 405 nm: photochemical advantages, localisation, phototoxicity and methods for calibration, *J. Neurosci. Methods*, 2009, **180**, 9–21.
15 Y. P. Zhang, N. Holbro and T. G. Oertner, Optical induction of plasticity at single synapses reveals input-specific accumulation of alphaCaMKII, *Proc. Natl. Acad. Sci. U. S. A.*, 2008, **105**, 12039–12044.
16 V. Nikolenko, K. E. Poskanzer and R. Yuste, Two-photon photostimulation and imaging of neural circuits, *Nat. Methods*, 2007, **4**, 943–950.
17 Y. Nong, Y. Q. Huang and M. W. Salter, NMDA receptors are movin' in, *Curr. Opin. Neurobiol.*, 2004, **14**, 353–361.
18 G. K. Dhami and S. S. G. Ferguson, Regulation of metabotropic glutamate receptor signaling, desensitization and endocytosis, *Pharmacol. Ther.*, 2006, **111**, 260–271.
19 R. Malinow, S. Rumpel, A. Zador and J. Ledoux, AMPA receptor trafficking and GluR1- Response, *Science*, 2005, **310**, 234–235.
20 R. C. Carroll, E. C. Beattie, M. von Zastrow and R. C. Malenka, Role of AMPA receptor endocytosis in synaptic plasticity, *Nat. Rev. Neurosci.*, 2001, **2**, 315–324.
21 T. C. Thiagarajan, M. Lindskog and R. W. Tsien, Adaptation to synaptic inactivity in hippocampal neurons, *Neuron*, 2005, **47**, 725–737.
22 K. Levitsky, M. D. Boersma, C. J. Ciolli and P. J. Belshaw, Exomechanism proximity-accelerated alkylations: Investigations of linkers, electrophiles and surface mutations in engineered cyclophilin-cyclosporin systems, *ChemBioChem*, 2005, **6**, 890–899.
23 K. Levitsky, C. J. Ciolli and P. J. Belshaw, Selective inhibition of engineered receptors *via* proximity-accelerated alkylation, *Org. Lett.*, 2003, **5**, 693–696.
24 D. A. Erlanson, J. A. Wells and A. C. Braisted, Tethering: fragment-based drug discovery, *Annu. Rev. Biophys. Biomol. Struct.*, 2004, **33**, 199–223.
25 J. J. Chambers, M. R. Banghart, D. Trauner and R. H. Kramer, Light-induced depolarization of neurons using a modified Shaker K(+) channel and a molecular photoswitch, *J. Neurophysiol.*, 2006, **96**, 2792–2796.
26 M. Banghart, K. Borges, E. Isacoff, D. Trauner and R. H. Kramer, Light-activated ion channels for remote control of neuronal firing, *Nat. Neurosci.*, 2004, **7**, 1381–1386.
27 M. Volgraf, P. Gorostiza, S. Szobota, M. R. Helix, E. Y. Isacoff and D. Trauner, Reversibly caged glutamate: a photochromic agonist of ionotropic glutamate receptors, *J. Am. Chem. Soc.*, 2007, **129**, 260–261.
28 J. Wang, N. A. Horenstein, C. Stokes and R. L. Papke, Tethered agonist analogs as site-specific probes for domains of the human alpha7 nicotinic acetylcholine receptor that differentially regulate activation and desensitization, *Mol. Pharmacol.*, 2010, **78**, 1012–1025.

29 R. H. Kramer and J. W. Karpen, Spanning binding sites on allosteric proteins with polymer-linked ligand dimers, *Nature*, 1998, **395**, 710–713.
30 S. S. Gallagher, C. Jing, D. S. Peterka, M. Konate, R. Wombacher, L. J. Kaufman, R. Yuste and V. W. Cornish, A trimethoprim-based chemical tag for live cell two-photon imaging, *ChemBioChem*, 2010, **11**, 782–784.
31 M. R. Banghart, A. Mourot, D. L. Fortin, J. Z. Yao, R. H. Kramer and D. Trauner, Photochromic blockers of voltage-gated potassium channels, *Angew. Chem., Int. Ed.*, 2009, **48**, 9097–9101.
32 J. A. Doorn and D. R. Petersen, Covalent adduction of nucleophilic amino acids by 4-hydroxynonenal and 4-oxononenal, *Chem.-Biol. Interact.*, 2003, **143–144**, 93–100.
33 K. M. Noh, H. Yokota, T. Mashiko, P. E. Castillo, R. S. Zukin and M. V. Bennett, Blockade of calcium-permeable AMPA receptors protects hippocampal neurons against global ischemia-induced death, *Proc. Natl. Acad. Sci. U. S. A.*, 2005, **102**, 12230–12235.
34 H. Kromann, S. Krikstolaityte, A. J. Andersen, K. Andersen, P. Krogsgaard-Larsen, J. W. Jaroszewski, J. Egebjerg and K. Stromgaard, Solid-phase synthesis of polyamine toxin analogues: potent and selective antagonists of Ca2+-permeable AMPA receptors, *J. Med. Chem.*, 2002, **45**, 5745–5754.
35 H. Tsubokawa, K. Oguro, T. Masuzawa, T. Nakaima and N. Kawai, Effects of a spider toxin and its analogue on glutamate-activated currents in the hippocampal CA1 neuron after ischemia, *J. Neurophysiol.*, 1995, **74**, 218–225.
36 M. Koike, M. Iino and S. Ozawa, Blocking effect of 1-naphthyl acetyl spermine on Ca2+-permeable AMPA receptors in cultured rat hippocampal neurons, *Neurosci. Res.*, 1997, **29**, 27–36.
37 G. Papageorgiou, D. Ogden and J. E. T. Corrie, An antenna-sensitized nitroindoline precursor to enable photorelease of L-glutamate in high concentrations, *J. Org. Chem.*, 2004, **69**, 7228–7233.
38 S. Surprenant and W. D. Lubell, 9-(4-Bromophenyl)-9-fluorenyl as a safety-catch nitrogen protecting group, *J. Org. Chem.*, 2006, **71**, 848–851.
39 J. Auernheimer, C. Dahmen, U. Hersel, A. Bausch and H. Kessler, Photoswitched cell adhesion on surfaces with RGD peptides, *J. Am. Chem. Soc.*, 2005, **127**, 16107–16110.
40 M. V. Kvach, A. V. Ustinov, I. A. Stepanova, A. D. Malakhov, M. V. Skorobogatyi, V. V. Shmanai and V. A. Korshun, A convenient synthesis of cyanine dyes: Reagents for the labeling of biomolecules, *Eur. J. Org. Chem.*, 2008, 2107–2117.
41 A. J. Geall, R. J. Taylor, M. E. Earll, M. A. Eaton and I. S. Blagbrough, Synthesis of cholesteryl polyamine carbamates: pK(a) studies and condensation of calf thymus DNA, *Bioconjugate Chem.*, 2000, **11**, 314–326.
42 M. Volgraf, P. Gorostiza, R. Numano, R. H. Kramer, E. Y. Isacoff and D. Trauner, Allosteric control of an ionotropic glutamate receptor with an optical switch, *Nat. Chem. Biol.*, 2005, **2**, 47–52.
43 P. T. H. Brackley, D. R. Bell, S. K. Choi, K. Nakanishi and P. N. R. Usherwood, Selective Antagonism of Native and Cloned Kainate and Nmda Receptors by Polyamine-Containing Toxins, *J. Pharmacol. Exp. Ther.*, 1993, **266**, 1573–1580.
44 P. Paoletti, L. Mony, J. N. C. Kew and M. J. Gunthorpe, Allosteric modulators of NR2B-containing NMDA receptors: molecular mechanisms and therapeutic potential, *Br. J. Pharmacol.*, 2009, **157**, 1301–1317.
45 N. Nagarajan, C. Quast, A. R. Boxall, M. Shahid and C. Rosenmund, Mechanism and impact of allosteric AMPA receptor modulation by the ampakine CX546, *Neuropharmacology*, 2001, **41**, 650–663.
46 J. J. Chambers and R. H. Kramer, Light-activated ion channels for remote control of neural activity, *Methods Cell Biol.*, 2008, **90**, 217–232.